https://doi.org/10.5194/acp-2020-174
Preprint. Discussion started: 24 March 2020

Atmospheric Chemistry and Physics Discussions

Contributions to OH reactivity from unexplored volatile organic compounds measured by PTR-ToF-MS– A case study in a suburban forest of the Seoul Metropolitan Area during KORUS-AQ 2016

Dianne Sanchez,[1] Roger Seco,[1*] Dasa Gu,[1] Alex Guenther,[1] John Mak,[2] Youngjae Lee,[3] Danbi Kim,[3] Joonyoung Ahn, [3] Don Blake,[4] Scott Herndon,[5] Daun Jeong,[1] John T. Sullivan,[6] Thomas Mcgee,[6] and Saewung Kim[1*]

1. Department of Earth System Science, University of California, Irvine, Irvine CA 92697, U.S.A.

2. School of Marine and Atmospheric Sciences, Stony Brooke University, Stony Brook, NY 11794, U.S.A.

3. National Institute of Environmental Research, Inchoen 22689, South Korea

4. Department of Chemistry, University of California, Irvine, Irvine CA 92697, U.S.A.

5. Aerodyne Research Inc., Billerica MA 01821, U.S.A.

6. NASA Goddard Space Flight Center, Chemistry and Dynamics Laboratory, Greenbelt, MD 20771, U.S.A.

* Now at: Terrestrial Ecology Section, Department of Biology, University of Copenhagen, Copenhagen, Denmark and
Center for Permafrost (CENPERM), Department of Geosciences and Natural Resource Management , University of Copenhagen, Copenhagen, Denmark

Corresponding author: saewung.kim@uci.edu, tel 1-949-824-4531

To be submitted to Atmospheric Chemistry and Physics

https://doi.org/10.5194/acp-2020-174
Preprint. Discussion started: 24 March 2020

Atmospheric Chemistry and Physics Discussions

Abstract

We report OH reactivity observations by a chemical ionization mass spectrometer – comparative reactivity method (CIMS-CRM) instrument in a suburban forest of the Seoul Metropolitan Area (SMA) during Korea US Air Quality Study (KORUS-AQ 2016) from mid-May to mid-June of 2016. A comprehensive observational suite was deployed to quantify reactive trace gases inside of the forest canopy including a high-resolution proton transfer reaction time of flight mass spectrometer (PTR-ToF-MS). An average OH reactivity of 30.7 ± 5.1 s^{-1} was observed, while the OH reactivity calculated from CO, NO + NO_2 (NO_x), ozone (O_3), sulfur dioxide (SO_2), and 14 volatile organic compounds (VOCs) was 11.8 ± 1.0 s^{-1}. An analysis of 346 peaks from the PTR-ToF-MS accounted for an additional 6.0 ± 2.2 s^{-1} of the total measured OH reactivity, leaving 42.0 % missing OH reactivity. The missing OH reactivity most likely comes from VOC oxidation products of both biogenic and anthropogenic origin.

https://doi.org/10.5194/acp-2020-174
Preprint. Discussion started: 24 March 2020

Atmospheric Chemistry and Physics Discussions

1. Introduction

Total OH reactivity (s^{-1}), the inverse of OH lifetime, is a measure of the total amount of reactive trace gases in the atmosphere in the scale of reactivity, which allow us to quantitatively evaluate our ability to constrain trace gases by comparing measurements of total OH reactivity with the OH reactivity calculated from a speciated reactive gas measurement dataset. The fraction of observed OH reactivity that cannot be reconciled by calculated OH reactivity is known as "missing OH reactivity" (Di Carlo et al., 2004;Goldstein and Galbally, 2007;Yang et al., 2016). A substantial amount of missing OH reactivity has consistently been reported in forest environments (30 - 80%). Di Carlo et al. (2004) conducted a study in a mixed forest near Pellston, Michigan where they reported missing OH reactivity larger than observational uncertainty. The authors concluded that the missing sources of reactivity were primary biogenic volatile organic compound (biogenic VOC, BVOC) emissions, as the degree of missing OH reactivity followed the temperature dependence of terpenoid emissions. In a boreal forest in Hyytiälä, Finland, Sinha et al. (2010) report a similar result with observed trace gases that account for only 50% of the measured OH reactivity. They argued that oxidation products of BVOCs alone could not account for the missing OH reactivity. Thus, they also concluded that primary emissions were more likely to be the source of missing OH reactivity and they further suggest that this could be the result of the contribution of small amounts of many reactive gases.

On the other hand, some studies have attributed the sources of the missing OH reactivity to unmeasured oxidation products of well-characterized BVOCs. Edwards et al. (2013) measured OH reactivity in a pristine tropical forest in the Sabah region of Borneo during the Oxidant and Particle Photochemical Processes (OP3) field campaign (Hewitt et al., 2010). This study implemented the Master Chemical Mechanism (MCMv3.2) (Saunders et al., 2003;Jenkin

https://doi.org/10.5194/acp-2020-174
Preprint. Discussion started: 24 March 2020


Atmospheric Chemistry and Physics Discussions

et al., 1997) into a box model framework to quantify potential contributions from unmeasured oxidation products. The model was constrained with VOCs such as isoprene, monoterpenes, and alkanes and alkenes and other observed trace gases such as NO + NO_2 (NO_x) and ozone (O_3). The authors reported that the model simulated oxygenated VOCs (OVOCs) could contribute 47.1% of the calculated OH reactivity – surpassing the contribution from isoprene, the primary emission of this ecosystem. It is notable that 30% of observed OH reactivity could not be accounted for by the box model simulations. After examining the comprehensive observational suite of VOCs, the authors determined that the most significant missing sources of OH reactivity were likely secondary multifunctional carbon compounds rather than primary BVOC emissions. Hansen et al. (2014) suggested that their observed missing OH reactivity were likely from unmeasured oxidation products during the Community Atmosphere-Biosphere INteraction EXperiment (CABINEX 2009) in Michigan. This notion was also consistent with findings reported by Kim et al. (2011) who measured OH reactivity of branch enclosures from four representative tree species in the forest canopy during the CABINEX study. They reconciled most of the measured OH reactivity of four representative tree species with well-known BVOCs, such as isoprene and monoterpenes. Finally, Nakashima et al. (2014) reported that 29.5% OH reactivity could not be reconciled by the speciated trace gas dataset during the Bio-hydro-atmosphere interactions of Energy, Aerosols, Carbon, H_2O, Organics and Nitrogen-Southern Rocky Mountain 2008 (BEACHON-SMR08) field campaign (Ortega et al., 2014). The campaign took place at the Manitou Experimental Forest (MEF) in Colorado, a ponderosa pine plantation dominated by primary BVOC emissions of 2-methyl-3-butene-2-ol (232-MBO) and monoterpenes (Ortega et al., 2014). The authors also reported that the missing OH reactivity was likely from BVOC oxidation products. In the same context, Kim et al. (2010) conducted PTR-

https://doi.org/10.5194/acp-2020-174
Preprint. Discussion started: 24 March 2020


Atmospheric Chemistry and Physics Discussions

MS mass spectrum analysis for both ambient air and branch enclosures at the MEF site. They reported more conspicuous unidentified signals on PTR-MS mass spectra in the ambient samples than those from branch enclosure samples at this site.

During the Southern Oxidant and Aerosol Study (SOAS) in 2013, Kaiser et al. (2016) used a comprehensive suite of VOC measurements at an isoprene dominant forest site in the southeastern US to examine the role of the OVOC species in missing reactive carbon. The authors used MCMv3.2 embedded in the University of Washington Chemical Box Model (UWCM) to compare OH reactivity from model-generated OVOCs to OH reactivity from measurements of OVOCs. There was no significant discrepancy between the average measured and calculated OH reactivity including observed trace gases and model calculated oxidation products of VOCs. However, it was noted that a small portion (1 s^{-1}) of observed OH reactivity could not be reconciled by the model calculation. As this fraction was not correlated to isoprene oxidation products, it was suggested that the missing OH reactivity may be due to unmeasured primary emissions. One caveat of this analysis pointed out by the authors was that the concentrations of the modeled first-generation isoprene oxidation products (e.g. MVK, MACR, isoprene hydroxy hydroperoxides (ISOPOOH), isoprene nitrates (ISOPN), and hydroperoxy aldehydes (HPALD)) were significantly overpredicted in the afternoon. Consequently, the uncertainty of the model calculation is likely to be much higher for the multi-generation oxidation products and their contributions to the OH reactivity contributions. This result highlights the uncertainty in relying solely on box-model results to assess OH reactivity.

This study examines the OH reactivity observations at Taehwa Research Forest (TRF) supersite from 15 May 2016 to 7 June 2016 during the Korea United States Air Quality Study 2016 (KORUS-AQ 2016) campaign. TRF (37 18’ 19.08” N 127 19’ 7.12” E, 162 m altitude) is

https://doi.org/10.5194/acp-2020-174
Preprint. Discussion started: 24 March 2020


Atmospheric Chemistry and Physics Discussions

operated by Seoul National University and located in Gwangju in the Gyunggi Province in South Korea (Kim et al., 2013b). The site is about 35 km southeast from the center of Seoul and borders the greater Seoul Metropolitan Area (SMA) with its population of 25.6 million. This geographical proximity to SMA results in a significant level of anthropogenic influence, particularly in elevated NO_x (Kim et al., 2016). Additionally, occasional pollution transport events occur at regional scales. Previous studies at the site have consistently highlighted the importance of BVOC photochemistry at TRF (Kim et al., 2016;Kim et al., 2013a;Kim et al., 2015). Isoprene and monoterpenes are the dominant OH sinks at the site among observed VOCs. The elevated NO_X accelerates the photochemical processing of VOCs (Kim et al., 2015). Thus, this site is an ideal natural laboratory to study contributions towards total OH reactivity from primary trace gas emissions from both natural and anthropogenic processes and their oxidation products. This motivated us to deploy a high-resolution proton transfer reaction time-of-flight mass spectrometer (PTR-ToF-MS) to quantify trace amounts of VOCs with unknown molecular structures by taking advantage of the universal sensitivity of hydronium ion chemistry towards reactive VOCs (Graus et al., 2010;Jordan et al., 2009a). Therefore, we intend to observationally constrain the contributions of conventionally unidentified or unmeasured VOCs towards OH reactivity.

2. Methods

2.1. Field Site

The Taehwa Research Forest is a Korean pine (*Pinus koraiensis*) plantation (300 m × 300 m) surrounded by a deciduous forest dominated by oak trees (Kim et al., 2013b). A flux tower (40 m height) at the center of TRF has air-sampling inlets at multiple heights (4 m, 8 m 12 m,

https://doi.org/10.5194/acp-2020-174
Preprint. Discussion started: 24 March 2020


Atmospheric Chemistry and Physics Discussions

and 16 m) below the canopy top (20 m). Each inlet consists of Teflon tubing (3/8" OD) with ~ 1 second of residence time. The trace gas dataset including VOCs presented is the average of concentrations measured at the inlets inside of the canopy as previous studies illustrate that there is no substantial vertical VOC gradients inside of the canopy (within 3 %, Kim et al. (2013b)). An air-conditioned instrument shack located at the base of the flux tower housed the PTR-ToF-MS for VOC measurements, a mini tunable infrared laser direct absorption spectroscopy (mini-TILDAS) instrument for HCHO, methane, and methanol measurements, and analyzers for carbon monoxide (CO), sulfur dioxide (SO_2), ozone (O_3), and meteorological measurements. The OH reactivity and NO_x analyzers were located in another nearby air-conditioned shack (3 m apart) and sampled air through an extended Teflon inlet line of 4 m (¼" OD) from the ground with a flow rate of 4 sLpm resulting in a 0.5 second residence time. The analytical characteristics of the instrumentation suite are summarized in Table 1. A ceilometer backscattering characterized boundary layer vertical structure at the site. The ceilometer analysis described by Sullivan et al. (2019) reveals the diurnal boundary layer height evolution, indicating a maximum in the afternoon around 1-3 km and a minimum in the early morning below 500 m.

2.2.OH Reactivity Measurements

A chemical ionization mass spectrometer – comparative reactivity method (CIMS-CRM) instrument was used to measure OH reactivity. The UCI CIMS-CRM system includes a chemical ionization mass spectrometer with a hydronium reagent ion. The CRM method measures total OH reactivity by quantifying the relative loss of pyrrole, a highly reactive gas ($k_{OH+\ pyrrole}$ = 1.45 × 10^{-10} cm^3 $molecule^{-1}$ s^{-1} at 298 K) that is rarely found in the atmosphere (Sinha et al., 2008b). Nitrogen gas flows through a bubbler full of ultrapure liquid chromatography mass spectrometer

https://doi.org/10.5194/acp-2020-174
Preprint. Discussion started: 24 March 2020


Atmospheric Chemistry and Physics Discussions

(LC-MS) grade water to produce water vapor. The water vapor then flows into a glass reactor where it is photolyzed into OH radicals by a mercury lamp (Pen-Ray® Light Source P/N 90-0012-01). The measurement uncertainty is 16.7% (1σ) with a limit of detection of 4.5 s^{-1} over 2 minutes (3σ).

The UCI CIMS-CRM instrument has been deployed on multiple occasions, including the Megacity Air Pollution Study (MAPS)-Seoul 2015 campaign that incorporated previous measurements at the TRF ground site during September 2015 (Sanchez et al., 2018;Kim et al., 2016). During the SOAS 2013 campaign, an ambient OH reactivity intercomparison study was conducted with laser induced fluorescence (LIF) system (Sanchez et al., 2018). The instrument intercomparison showed that the OH reactivity measurements from the CRM and LIF instruments generally agreed within the analytical uncertainty. An average of 16% difference between the techniques was noted in the late afternoons where the CRM measurements were lower than those from LIF. As discussed in Sanchez et al. (2018), this is likely caused by the difference in sampling strategies, as the CRM measurements relied on a lengthy Teflon inlet (15 m) while the LIF directly sampled air at the top of a walk up tower. As mentioned above, at TRF we used a shorter inlet line to minimize residence time and avoid inlet line loss.

An extensive intercomparison study was conducted by Fuchs et al. (2017) with various OH reactivity measurement techniques that highlighted potential analytical artifacts in the CRM technique. These artifacts have all been examined and preventive measures have been implemented in the UCI CIMS-CRM system deployed at TRF. This included a laboratory-built catalytic converter (Pt-wool at 350 °C) that minimized the interferences due to changes in air to prevent the interference from the difference in humidity for the zero air characterizations. Additionally, interference from the OH recycling reaction of HO_2 with NO in the glass chamber

https://doi.org/10.5194/acp-2020-174
Preprint. Discussion started: 24 March 2020


Atmospheric Chemistry and Physics Discussions

was prevented by removing OH reactivity data points that corresponded with ambient NO levels that exceeded 5 ppb to reflect results from a laboratory characterization study (Sanchez et al., 2018). Finally, we performed multi-point calibrations with a propene mixture using a NIST traceable gas standard (AirLiquide LLC, 0.847 ppm) during the field campaign to avoid any circumstances where the pseudo first-order reaction regime is not established. Detailed calibration procedures for the OH reactivity system including laboratory multi-component calibration results can be found in Sanchez et al. (2018).

2.3.PTR-ToF-MS Measurements

A high-resolution PTR-TOF-MS (Ionicon Analytik GmbH) (de Gouw and Warneke, 2007), (Jordan et al., 2009b) was deployed at the TRF site. The instrument was operated with a drift tube temperature of 60 °C, 560 V drift voltage, and 2.27 mbar drift tube to maintain E/N of 126 Td. Background checks were manually conducted about three times a day for a 10-minute duration by scrubbing the ambient air through a catalytic convertor (Pt-wool maintained at 350°C). The detectable peaks from the ambient spectra were assessed by subtracting the background spectrum. The instrument was calibrated with a gas mixture manufactured by Apel-Riemer Environmental Inc. The mixture contains ~ 1 ppmv of acetaldehyde, acetone, isoprene, methyl vinyl ketone, methacrolein, benzene, methly ethyl ketone, toluene, o-xylene, and α-pinene. The concentration of the compounds were assessed in the Blake Lab at University of California, Irvine, who also conducted the airborne VOC analysis using whole air samples during the KORUS-AQ campaign on the NASA DC-8 (Colman et al., 2001).

A mass range of m/z 40 to m/z 267 was analyzed from the recorded PTR-ToF-MS mass spectra. An automatic mass scale calibration was conducted every 5 minutes on the data

https://doi.org/10.5194/acp-2020-174
Preprint. Discussion started: 24 March 2020

Atmospheric Chemistry and Physics Discussions

averaged over 30 seconds. The raw PTR-ToF-MS data were processed using the PTRwid software described by Holzinger (2015). We normalized the mass peaks by 10^6 reagent ion counts (H_3O^+). As the majority of the VOC mass peaks could not be directly calibrated, we determined the VOC sensitivities using equation 1 (Eq 1). We obtained a VOC mixing ratio (ppb_{VOC}) by multiplying mass discrimination corrected normalized counts for each VOC ($ncps_{VOC}$) by their proton transfer reaction rate coefficient value (k_{VOC}) (Cappellin et al., 2012). The benzene calibration factor was used to calculate mixing ratios by applying its proton transfer reaction rate coefficient ($k_{benzene}$) and sensitivity (ncps ppb^{-1}) for the available compounds.

$$ppb_{VOC} = \frac{ncps_{VOC}}{11.94\frac{ncps_{benzene}}{ppb}} \times \frac{k_{benzene}}{k_{VOC}} \quad \text{Eq. 1}$$

For the mass peaks where specific proton transfer reaction rates were unavailable, we estimated the mixing ratios by applying a proton transfer reaction rate coefficient (k_{H3O+}) of 3.00×10^{-9} cm^3 s^{-1}, the default value for PTRwid calculations. The spectra had a limit of detection of tens of ppt for a 30 second average. The calibrated compounds had a range of detection limits as low as 3.7 ppt for α-pinene and as high as 48 ppt for toluene.

2.4. *OH Reactivity Calculation*

OH reactivity was calculated from the concentrations of all the compounds observed by the instrumental suite described in Table 1. The original data can be found in the KORUS-AQ 2016 data archive at https://korus-aq.larc.nasa.gov/. A total of 360 mass peaks measured by the PTR-ToF-MS were analyzed above the background (3 σ or above) to assess their contribution to the calculated OH reactivity. Fourteen of the mass peaks were identified as VOCs commonly

https://doi.org/10.5194/acp-2020-174
Preprint. Discussion started: 24 March 2020


Atmospheric Chemistry and Physics Discussions

233 reported for PTR-MS measurements (Table 1), leaving 346 unidentified peaks. These remaining
234 mass peaks were grouped into three categories in order to estimate their possible OH reactivity
235 contribution.

236 Category I included mass peaks for which the PTRwid software calculated a molecular
237 formula. OH reaction rate coefficients for the individual peaks were obtained from the National
238 Institute for Standards and Technology (NIST) Webbook library. If the information was
239 unavailable from the NIST Webbook database, a structure-reactivity relationship described by
240 Kwok and Atkinson (1995) was applied to obtain reaction rate coefficients. This is an empirical
241 calculation system to estimate k_{OH} based upon the number of carbons and the functional groups
242 of given VOCs. The framework is able to calculate k_{OH} within a factor of two according to a
243 thorough assessments presented in Kwok and Atkinson (1995). However, the authors discourage
244 the application of the framework to compounds that were not examined in the study such as
245 halogenated compounds. Although halogenated compounds are not included in this study, one
246 should be aware of a potentially significant uncertainty.

247 Category II included mass peaks for which the PTRwid software could not assess an
248 exact molecular composition due to uncertainty in the data processing system. Nonetheless, this
249 group of compounds illustrated a positive correlation with either anthropogenic (benzene,
250 toluene) or biogenic (MVK+MACR and monoterpenes) VOCs. Category II compounds are
251 further grouped into subcategories corresponding to these two main VOC sources.
252 OH reaction rate constants (k_{OH}) were estimated with equations based on the relationship
253 between the *m/z* and the k_{OH} of compounds in Table 1 (Figure S1). The compounds were grouped
254 into 5 *m/z* bins and the average k_{OH} of each bin was calculated. The green triangles represent 5
255 *m/z* binned averages from these compounds plotted with their respective average k_{OH}. This

https://doi.org/10.5194/acp-2020-174
Preprint. Discussion started: 24 March 2020


Atmospheric Chemistry and Physics Discussions

256 approach can be justified by the fact that the reaction constants of VOCs towards OH tend to
257 increase as a function of molecular mass within functional groups (Kwok and Atkinson,
258 1995;Atkinson, 1987). The y-intercepts of the linear regressions were assessed using the k_{OH}
259 values of the biogenic or anthropogenic compounds and their masses.

260 Category III included mass peaks with very low mixing ratios (average = 4.8 ppt ±19.5
261 ppt) that were above the limit of detection. We applied a k_{OH} corresponding to the dark green
262 best-fit line in Figure S1 to these peaks. The y-intercept of the dark green line was based on that
263 of acetaldehyde, as it was the lowest mass compound used for the OH reactivity calculations in
264 this study.

265

266 **3. Results and Discussion**

267 An average OH reactivity of 30.7 ± 5.1 s^{-1} was observed from 15 May – 7 June 2016
268 (Figure 1). This was within the range of OH reactivity observed in urban regions (10 - 33 s^{-1}).
269 (Kovacs et al., 2003;Ren et al., 2003;Sinha et al., 2008a;Dolgorouky et al., 2012;Whalley et al.,
270 2016;Kim et al., 2016;Yang et al., 2017) and in the range of previously reported observations
271 and model calculations at the TRF site (~15 - 35 s^{-1}) (Kim et al., 2016;Kim et al., 2015). The
272 total calculated OH reactivity of 11.8 ± 1.0 s^{-1} from the measured compounds in Table 1 resulted
273 in 63.3% missing OH reactivity. However, an additional OH reactivity of 6.0 ± 2.2 s^{-1} was
274 further calculated from the reactivity of the VOCs in Categories I – III. The contribution lowered
275 the missing OH reactivity level to 42% of the measured OH reactivity. Kim et al. (2016) had
276 previously measured an average OH reactivity of 16.5 s^{-1} at TRF during the MAPS-Seoul
277 campaign from 1 September – 15 September 2015, a substantially lower level then what we
278 report during this springtime study. Although small alkanes and alkenes such as ethane, ethene,

https://doi.org/10.5194/acp-2020-174
Preprint. Discussion started: 24 March 2020


Atmospheric Chemistry and Physics Discussions

propane and propene were not observed on the site, we utilized the dataset from the NASA DC-8 that flew at 700 m above the site, which indicates that their contribution was consistently small (~ 0.7 s^{-1} in average).

The difference can be attributed to the notably higher reactive trace gas loadings during KORUS-AQ compared to the TRF measurements during MAPS-Seoul. The NO_x, benzene, and toluene concentrations were 3 times higher during KORUS-AQ and CO was 1.4 times higher (Figure S2). Although the average isoprene concentrations were similar between the two campaigns, MVK and MACR concentrations during KORUS-AQ were ~3 times higher, illustrating a higher oxidative environment. There was a persistently high MVK+MACR to isoprene ratio of 1.8 during the KORUS-AQ campaign at TRF. This ratio was similar to the value reported during the summer in a moderately polluted forest in the Pearl River Delta that was attributed to a strong atmospheric oxidation capacity (Gong et al., 2018). The missing OH reactivity during KORUS-AQ was generally much higher than levels reported during urban observations (up to 50% missing OH reactivity) (Kovacs et al., 2003;Ren et al., 2003;Sinha et al., 2008a;Dolgorouky et al., 2012;Whalley et al., 2016;Kim et al., 2016;Yang et al., 2017) and within the range of previously reported values in forest regions where as much as 80% missing OH reactivity has been reported (Kim et al., 2016;Di Carlo et al., 2004;Nolscher et al., 2012;Edwards et al., 2013;Nolscher et al., 2016;Ramasamy et al., 2018;Nakashima et al., 2014).

Figure 2 shows the diurnal average of measured, calculated, and missing OH reactivity from 15 May – 7 June 2016. Isoprene was the largest contributor to VOC OH reactivity in the afternoon and the early evening (36% of the calculated OH reactivity in the evening), consistent with the previous studies conducted in this site (Kim et al., 2016;Kim et al., 2013b;Kim et al., 2015). Among all the trace gases, the largest average contributor to the calculated OH reactivity

https://doi.org/10.5194/acp-2020-174
Preprint. Discussion started: 24 March 2020


Atmospheric Chemistry and Physics Discussions

was NO_x, which contributed 18.2% (5.6 s^{-1}) to the measured OH reactivity. The NO_x contribution to OH reactivity is higher during the morning and evening rush hours and at a minimum in the afternoon, which has been reported consistently in previous reports conducted near megacities (Kovacs et al., 2003;Mao et al., 2010;Dolgorouky et al., 2012;Ren et al., 2003;Shirley et al., 2006). Enhanced OH reactivity during the morning or night and minimum OH reactivity during the afternoon have been reported in urban areas (Kovacs et al., 2003;Ren et al., 2006;Shirley et al., 2006;Dolgorouky et al., 2012;Mao et al., 2010;Whalley et al., 2016). On the other hand, strong light-sensitive biogenic emissions (e.g. isoprene) result in a maximum observed OH reactivity in the afternoon in forested regions (Ren et al., 2006;Sinha et al., 2012;Edwards et al., 2013;Hansen et al., 2014;Zannoni et al., 2017;Nolscher et al., 2016) . One exception is an OH reactivity observation conducted in Hyytiälä, a forested site that has low isoprene levels, by Sinha et al. (2010). They attributed a flat diurnal OH reactivity variation to the interplay between high daytime emissions and low nighttime boundary layer height. In urban environments, it is mostly anthropogenic trace gases such as aromatics and OVOCs that contribute to OH reactivity. These compounds have a longer lifetime compared to the diurnal boundary layer evolution. This leads to the accumulation of such compounds in the shallow boundary layer during the night. On the other hand, strong emissions of reactive BVOCs in deciduous forest regions enhance OH reactivity during the daytime but then quickly react away. Very subtle diurnal differences observed in this study (Figure 2), therefore, can be understood as the competitive influences of both anthropogenic and biogenic compounds to the OH reactivity.

As described in detail in Sullivan et al. (2019) and Jeong et al. (2019), a strong regional stagnation episode occurred during the KORUS-AQ campaign between May 17 – 23. Later, the Korean Peninsula was affected by a period of continental pollution outflow between May 28 and

https://doi.org/10.5194/acp-2020-174
Preprint. Discussion started: 24 March 2020


Atmospheric Chemistry and Physics Discussions

June 1. The diurnal averages of the two periods and their calculated OH reactivity are presented in Figure 3. It is notable that there is very little difference in the observed OH reactivity between the two distinct periods in terms of the amount of OH reactivity and its diurnal pattern (Figure 4). Furthermore, no significant variance of the different classes of reactive gases such as criteria air pollutants (CO, NO_x, O_3, and SO_2), OVOCs (acetone, acetaldehyde, formaldehyde, methylglyoxal, methanol, methyl ethyl ketone), aromatics (benzene, toluene, xylenes, styrene, benzaldehyde, trimethylbenzenes), and BVOCs (isoprene, monoterpenes, sesquiterpenes, MVK+MACR) was observed during the different periods (Figure 5). These different classes of reactive gases generally differed by less than 10% during the two periods from the overall campaign. This observation shows that the presence of reactive gases is mostly controlled by relatively short-lived compounds determined by local emissions and their oxidation products.

The diurnal variation behavior of each chemical class reflects the chemical lifetime of the compounds (e.g. aromatics vs BVOCs). The calculated OH reactivity from OVOCs does not show a strong diurnal variation. This reflects the fact that OVOCs are mostly generated or emitted during the daytime and their lifetime is generally longer than their precursors, which allows nocturnal accumulation due to the absence of OH. The differences in the diurnal variation of different classes of reactive gases can also be used to interpret the origin of the compounds in Categories I-III as presented in Figure 6. The diurnal variations of Category I resemble those of relatively long-lived chemical species with a distinct nocturnal accumulation pattern. This diurnal pattern has been previously reported for both anthropogenic VOCs such as toluene and benzene and temperature dependent monoterpenes such as α-pinene. It is notable that the diurnal pattern is enhanced during the stagnation period during early morning hours. This enhancement is also seen in the aromatic trace gases particularly during the stagnation period (Figure 5b).

https://doi.org/10.5194/acp-2020-174
Preprint. Discussion started: 24 March 2020


Atmospheric Chemistry and Physics Discussions

348 Indeed, there are both biogenic and anthropogenic contributions towards the Category I
349 compounds, which contribute an average of 3.8 s^{-1} to the OH reactivity assessment, the largest
350 amount among the three categories (Figure 6a). The largest contributors to Category I, which
351 appear to be from a mixture of biogenic and anthropogenic sources, include *m/z* 89.060, 101.06,
352 and 101.096, and they contributed 0.3 s^{-1}, 0.2 s^{-1}, and 0.2 s^{-1}, respectively. The m/z 89.060 had a
353 molecular formula of $C_4H_8O_2H^+$ and was correlated to the anthropogenic compounds such as
354 benzene and toluene. The *m/z* 101.06 peak had the molecular formula of $C_5H_8O_2H^+$ and had a
355 diurnal variation similar to that of MVK + MACR. This mass peak has been previously
356 identified in laboratory (Zhao et al., 2004) and field (Williams et al., 2001) studies as the C_5
357 hydroxy carbonyl, an isoprene oxidation product. Results from an indoor chamber
358 photooxidation experiment conducted by Lee et al. (2006) showed that *m/z* 101 is a common
359 fragment of unidentified oxidation products of monoterpenes, sesquiterpenes, and isoprene. Lee
360 et al. (2006) also reported that this mass peak also composed over 5% of the fragments of
361 unidentified α- humulene and linalool oxidation products. The molecular formula of this peak is
362 $C_6H_{12}OH^+$, and it has been identified in previous studies as C_6 carbonyls (Koss et al., 2017) or
363 hexanal (Brilli et al., 2014;Rinne et al., 2005). Furthermore, *m/z* 99.044 and 113.023 were also
364 among the highest contributors to Category I and were correlated with MVK and MACR. The
365 *m/z* 99 was previously reported to be a fragment ion of unidentified terpene oxidation products in
366 a chamber experiment (Lee et al., 2006). The *m/z* 113 was observed by a PTR-MS in a
367 Ponderosa pine forest in central California by Holzinger et al. (2005). In this case, it was formed
368 within the canopy from the rapid oxidation of terpinolene, myrcene, and α-terpinene.
369 Furthermore, *m/z* 113 was observed to come from the photooxidation and ozonolyis of multiple
370 terpenes in two indoor chamber studies by Lee et al. (2006). The m/z 113 composed over 5% of

https://doi.org/10.5194/acp-2020-174
Preprint. Discussion started: 24 March 2020


Atmospheric Chemistry and Physics Discussions

371 the oxidation product fragments of myrcene and verbenone. Finally, m/z 83.085 had the
372 molecular formula of $C_6H_{11}^+$ and was correlated to benzene. Multiple studies have identified this
373 peak as cyclohexane, methyl-cyclopentane, or methylcyclohexane, typically found in areas rich
374 in oil and gas (Koss et al., 2017;Gueneron et al., 2015;Yuan et al., 2014). In summary, both the
375 gross diurnal pattern and the individual peak analyses consistently illustrates that both
376 anthropogenic and biogenic compounds comprise Category I, the largest contributor to the
377 previously unexplored compounds in the PTR-ToF-MS spectrum at this research site.
378 Category II contributed an average of 0.3 s^{-1} to the calculated OH reactivity, the lowest
379 amount for the three Categories (Figure 6b). The compounds in category II appear to correlate to
380 either BVOCs or acetone, depending on the time period. In Figure 6b, the maximum during the
381 transport period is enhanced to about 0.2 s^{-1} higher than the overall campaign and shifted about 3
382 hours later to ~4:00 PM. The OH reactivity calculated from Category II is strongly correlated to
383 MVK + MACR ($r^2 = 0.82$) during this period as well. On the other hand, during the stagnation
384 period the average OH reactivity from Category II correlates more strongly with acetone ($r^2 =$
385 0.62) than with MVK +MACR ($r^2 = 0.28$). In fact, six of the highest contributors to Category II
386 (Figure 6b) are more strongly correlated to acetone ($r^2 > 0.40$) during the stagnation period
387 compared to the transport period. The sources of acetone can be either biogenic or
388 anthropogenic. Biogenic sources include direct emissions from plants or their oxidation products
389 and plant decay (Jacob et al., 2002;Seco et al., 2007). Anthropogenic sources of acetone include
390 vehicular emissions, solvent use, and the oxidation of other anthropogenic VOCs (Jacob et al.,
391 2002). Therefore, this illustrates that the compounds in Category II also have a complex source
392 profile of both biogenic and anthropogenic origin.

https://doi.org/10.5194/acp-2020-174
Preprint. Discussion started: 24 March 2020


Atmospheric Chemistry and Physics Discussions

393 Category III contributed 1.9 s^{-1} to the calculated OH reactivity (Figure 6c). The six
394 highest contributors out of 236 mass peaks contributed a total of 0.43 s^{-1} of the calculated OH
395 reactivity. Overall, Category III compounds had no strong correlations to isoprene,
396 MVK+MACR, benzene, or toluene during either the stagnation or transport periods. However,
397 Category III compounds were highly correlated to methylglyoxal (r^2 = 0.85, 0.82, and 0.78 for
398 the stagnation, transport, and overall period, respectively), one of the measured OVOCs. A
399 global modeling study illustrated that methylglyoxal is mainly produced from isoprene oxidation
400 processes and the second most important source is acetone oxidation (Fu et al., 2008). In
401 addition, aromatics and alkenes are also known to produce methylglyoxal through atmospheric
402 oxidation processes (Henry et al., 2012). As TRF is a high aromatics and high isoprene
403 environment, the source profile of methyl glyoxal in the region is likely complex, which can be
404 applied to interpret the source of the Category III compounds.
405 Overall, the OH reactivity estimates from Categories I – III contributed an average of 6.0
406 ± 2.2 s^{-1} to the calculated OH reactivity. In summary, there is consistency that both
407 anthropogenic and the biogenic contributions need to be further studied in the PTR-ToF-MS
408 spectrum. Furthermore, by adding this additional signal from Category I, II, and III, VOC
409 contribution to calculated OH reactivity (11.0 s^{-1}) becomes larger than that (6.8 s^{-1}) from criteria
410 air pollutants (CO, NO_x, SO_2 and O_3). This should be considered when evaluating ozone
411 production regimes (Kim et al., 2018).
412 Even with the inclusion of the additional peaks to the calculated OH reactivity, we still
413 find a missing OH reactivity of 42%. Thus, it is important to investigate the origin of this
414 missing fraction. A correlation can be observed between missing OH reactivity in percentage and
415 OH reactivity from NO_X (R2 = 0.5, Figure 7 A) but not between OH reactivity from NO_x and

https://doi.org/10.5194/acp-2020-174
Preprint. Discussion started: 24 March 2020


Atmospheric Chemistry and Physics Discussions

absolute missing OH reactivity (s^{-1}) (R2 = 0.2, Figure 7 B). This leads us to speculate that there is a consistent presence of unquantified trace gases causing missing OH reactivity. As NO_x illustrates a conspicuous temporal variation that appears to correlate with the fraction of missing OH reactivity, while observed OH reactivity and calculated OH reactivity from VOCs indicate a less pronounced diurnal difference.

Finally, unaccounted for uncertainty associated with the reaction rate constant estimations described in the method section should be also further explored. For example, to reconcile the averaged missing OH reactivity during the day (10 s^{-1}), it requires ~ 60 ppm of methane but only ~ 4 ppb of isoprene. This clearly demonstrates the importance of rate constant estimation. Indeed, if we apply the reaction rate constant of isoprene with OH (k_{OH} = 1 × 10^{-10} cm^3 $molecule^{-1}$ s^{-1}at 298 K) to Category II and Category III compounds, then the observed OH reactivity is fully reconciled (Figure S3). Proton ion chemistry may have an intrinsic limitation to quantify highly oxidized OVOCs. Moreover, due to the different inlet configurations for OH reactivity and VOC observations, their contributions towards observed and calculated OH reactivity may not have been consistently evaluated. Therefore, a comprehensive analysis along with a dataset from other instrumentation is necessary towards reconciling missing OH reactivity with observational constraints. Finally, it is highly plausible that we may double count for fragmented molecules in the mass spectrum. Although it would not affect concentration evaluation as the intensity of ion signals from the fragmented molecules would be fully accounted for by adding parent ion and fragmented ion signals, the OH reactivity calculated from the fragmented ions is susceptible to underestimation from the assumption that k_{OH} positively correlates with molecular masses.

https://doi.org/10.5194/acp-2020-174
Preprint. Discussion started: 24 March 2020


Atmospheric Chemistry and Physics Discussions

4. *Summary*

We present OH reactivity observations at a suburban forest site during the KORUS-AQ field campaign. A comprehensive trace gas dataset including 14 VOCs quantified by PTR-ToF-MS is used to calculate OH reactivity, which only accounts for 36.7 % of the averaged observed OH reactivity.

This study presents a detailed methodology for retrieving OH reactivity contributions from all of the peaks of the PTR-ToF-MS mass spectrum. This decreases the amount of missing OH reactivity as the majority of them have not been accounted towards calculated OH reactivity in previous studies. First, we converted the raw signals to concentrations using a constant proton transfer reaction rate (3×10^{-9} cm^3 s^{-1}). Then, we grouped the previously unaccounted peaks into three categories to estimate reaction constants for each compound. The contributions of the unaccounted peaks in the mass spectrum account for a calculated OH reactivity of ~ 6 s^{-1}, which decreases missing OH reactivity from 63.3 % to 42.0 %. It is noteworthy that the diurnal variations of observed OH reactivity and calculated OH reactivity from the various groups of trace gases does not have a high variability during the field campaign even though there were several synoptic meteorological configuration changes. This suggests that the reactive trace gas loading is mostly determined by local emission and oxidation processes not influenced by the synoptic meteorological conditions.

In conclusion, this study highlights PTR-ToF-MS as a tool for observationally constraining missing OH reactivity. Further study is required particularly towards characterizing proton reaction rate constants and reaction constants with OH for the many unknown compounds detected on PTR-ToF-MS. In addition, other mass spectrometry techniques, such as nitrate or iodine ion chemistry systems, should be utilized in future studies to complement the PTR

https://doi.org/10.5194/acp-2020-174
Preprint. Discussion started: 24 March 2020

Atmospheric Chemistry and Physics Discussions

technique, which is sensitive to volatile to semi volatile VOCs, to quantify lower volatility compounds and comprehensively constrain OH reactivity contributions from VOCs.

Acknowledgements

This study is supported by NASA (NNX15AT90G) and NIER. We highly appreciate NASA ESPO for logistical support. Taehwa Research Forest is operated by College of Agriculture and Life Sciences at Seoul National University.

Data Availability

Data is available at: https://korus-aq.larc.nasa.gov/

References

Atkinson, R.: A Structure-Activity Relationship for the Estimation of Rate Constants for the Gas-Phase Reactions of Oh Radicals with Organic-Compounds, International Journal of Chemical Kinetics, 19, 799-828, DOI 10.1002/kin.550190903, 1987.

Brilli, F., Gioli, B., Ciccioli, P., Zona, D., Loreto, F., Janssens, I. A., and Ceulemans, R.: Proton Transfer Reaction Time-of-Flight Mass Spectrometric (PTR-TOF-MS) determination of volatile organic compounds (VOCs) emitted from a biomass fire developed under stable nocturnal conditions, Atmospheric Environment, 97, 54-67, 10.1016/j.atmosenv.2014.08.007, 2014.

Cappellin, L., Karl, T., Probst, M., Ismailova, K., Winkler, P. M., Soukoulis, C., Aprea, E., Mark, T. D., Gasperi, F., and Biasioli, F.: On quantitative determination of volatile organic compound concentrations using proton transfer reaction Time-of-Flight Mass Spectrometry, Environment Science & Technology, 46, 2012.

Colman, J. J., Swanson, A. L., Meinardi, S., Sive, B. C., Blake, D. R., and Rowland, F. S.: Description of the analysis of a wide range of volatile organic compounds in whole air samples collected during PEM-Tropics A and B, Analytical Chemistry, 73, 3723-3731, 2001.

https://doi.org/10.5194/acp-2020-174
Preprint. Discussion started: 24 March 2020

Atmospheric Chemistry and Physics Discussions

491 de Gouw, J., and Warneke, C.: Measurements of volatile organic compounds in the earth's
492 atmosphere using proton-transfer-reaction mass spectrometry, Mass Spectrom Rev, 26, 223-257,
493 10.1002/mas.20119, 2007.
494 Di Carlo, P., Brune, W. H., Martinez, M., Harder, H., Lesher, R., Ren, X. R., Thornberry, T.,
495 Carroll, M. A., Young, V., Shepson, P. B., Riemer, D., Apel, E., and Campbell, C.: Missing OH
496 reactivity in a forest: Evidence for unknown reactive biogenic VOCs, Science, 304, 722-725, Doi
497 10.1126/Science.1094392, 2004.
498 Dolgorouky, C., Gros, V., Sarda-Esteve, R., Sinha, V., Williams, J., Marchand, N., Sauvage, S.,
499 Poulain, L., Sciare, J., and Bonsang, B.: Total OH reactivity measurements in Paris during the
500 2010 MEGAPOLI winter campaign, Atmospheric Chemistry and Physics, 12, 9593-9612, Doi
501 10.5194/Acp-12-9593-2012, 2012.
502 Edwards, P. M., Evans, M. J., Furneaux, K. L., Hopkins, J., Ingham, T., Jones, C., Lee, J. D.,
503 Lewis, A. C., Moller, S. J., Stone, D., Whalley, L. K., and Heard, D. E.: OH reactivity in a South
504 East Asian tropical rainforest during the Oxidant and Particle Photochemical Processes (OP3)
505 project, Atmospheric Chemistry and Physics, 13, 9497-9514, Doi 10.5194/Acp-13-9497-2013,
506 2013.
507 Fu, T. M., Jacob, D. J., Wittrock, F., Burrows, J. P., Vrekoussis, M., and Henze, D. K.: Global
508 budgets of atmospheric glyoxal and methylglyoxal, and implications for formation of secondary
509 organic aerosols, Journal of Geophysical Research-Atmospheres, 113, 2008.
510 Fuchs, H., Novelli, A., Rolletter, M., Hofzumahaus, A., Pfannerstill, E. Y., Kessel, S., Edtbauer,
511 A., Williams, J., Michoud, V., Dusanter, S., Locoge, N., Zannoni, N., Gros, V., Truong, F.,
512 Sarda-Esteve, R., Cryer, D. R., Brumby, C. A., Whalley, L. K., Stone, D., Seakins, P. W., Heard,
513 D. E., Schoemaecker, C., Blocquet, M., Coudert, S., Batut, S., Fittschen, C., Thames, A. B.,
514 Brune, W. H., Ernest, C., Harder, H., Muller, J. B. A., Elste, T., Kubistin, D., Andres, S., Bohn,
515 B., Hohaus, T., Holland, F., Li, X., Rohrer, F., Kiendler-Scharr, A., Tillmann, R., Wegener, R.,
516 Yu, Z. J., Zou, Q., and Wahner, A.: Comparison of OH reactivity measurements in the
517 atmospheric simulation chamber SAPHIR, Atmospheric Measurement Techniques, 10, 4023-
518 4053, 2017.
519 Goldstein, A. H., and Galbally, I. E.: Known and unexplored organic constituents in the earth's
520 atmosphere, Environmental Science & Technology, 41, 1514-1521, 2007.
521 Gong, D. C., Wang, H., Zhang, S. Y., Wang, Y., Liu, S. C., Guo, H., Shao, M., He, C. R., Chen,
522 D. H., He, L. Y., Zhou, L., Morawska, L., Zhang, Y. H., and Wang, B. G.: Low-level
523 summertime isoprene observed at a forested mountaintop site in southern China: implications for
524 strong regional atmospheric oxidative capacity, Atmospheric Chemistry and Physics, 18, 14417-
525 14432, 10.5194/acp-18-14417-2018, 2018.
526 Graus, M., Muller, M., and Hansel, A.: High Resolution PTR-TOF: Quantification and Formula
527 Confirmation of VOC in Real Time, J Am Soc Mass Spectr, 21, 1037-1044, 2010.
528 Gueneron, M., Erickson, M. H., VanderSchelden, G. S., and Jobson, B. T.: PTR-MS
529 fragmentation patterns of gasoline hydrocarbons, International Journal of Mass Spectrometry,
530 379, 97-109, 10.1016/j.ijms.2015.01.001, 2015.
531 Hansen, R. F., Griffith, S. M., Dusanter, S., Rickly, P. S., Stevens, P. S., Bertman, S. B., Carroll,
532 M. A., Erickson, M. H., Flynn, J. H., Grossberg, N., Jobson, B. T., Lefer, B. L., and Wallace, H.
533 W.: Measurements of total hydroxyl radical reactivity during CABINEX 2009-Part 1: field
534 measurements, Atmospheric Chemistry and Physics, 14, 2923-2937, 10.5194/acp-14-2923-2014,
535 2014.

https://doi.org/10.5194/acp-2020-174
Preprint. Discussion started: 24 March 2020

536 Henry, S. B., Kammrath, A., and Keutsch, F. N.: Quantification of gas-phase glyoxal and
537 methylglyoxal via the Laser-Induced Phosphorescence of (methyl)GLyOxal Spectrometry
538 (LIPGLOS) Method, Atmospheric Measurement Techniques, 5, 181-192, 10.5194/amt-5-181-
539 2012, 2012.
540 Hewitt, C. N., Lee, J. D., MacKenzie, A. R., Barkley, M. P., Carslaw, N., Carver, G. D.,
541 Chappell, N. A., Coe, H., Collier, C., Commane, R., Davies, F., Davison, B., Di Carlo, P., Di
542 Marco, C. F., Dorsey, J. R., Edwards, P. M., Evans, M. J., Fowler, D., Furneaux, K. L.,
543 Gallagher, M., Guenther, A., Heard, D. E., Helfter, C., Hopkins, J., Ingham, T., Irwin, M., Jones,
544 C., Karunaharan, A., Langford, B., Lewis, A. C., Lim, S. F., MacDonald, S. M., Mahajan, A. S.,
545 Malpass, S., McFiggans, G., Mills, G., Misztal, P., Moller, S., Monks, P. S., Nemitz, E., Nicolas-
546 Perea, V., Oetjen, H., Oram, D. E., Palmer, P. I., Phillips, G. J., Pike, R., Plane, J. M. C., Pugh,
547 T., Pyle, J. A., Reeves, C. E., Robinson, N. H., Stewart, D., Stone, D., Whalley, L. K., and Yin,
548 X.: Overview: oxidant and particle photochemical processes above a south-east Asian tropical
549 rainforest (the OP3 project): introduction, rationale, location characteristics and tools,
550 Atmospheric Chemistry and Physics, 10, 169-199, 10.5194/acp-10-169-2010, 2010.
551 Holzinger, R., Lee, A., Paw, K. T., and Goldstein, A. H.: Observations of oxidation products
552 above a forest imply biogenic emissions of very reactive compounds, Atmospheric Chemistry
553 and Physics, 5, 67-75, DOI 10.5194/acp-5-67-2005, 2005.
554 Holzinger, R.: PTRwid: A new widget tool for processing PTR-TOF-MS data, Atmospheric
555 Measurement Techniques, 8, 3903-3922, 10.5194/amt-8-3903-2015, 2015.
556 Jacob, D. J., Field, B. D., Jin, E. M., Bey, I., Li, Q. B., Logan, J. A., Yantosca, R. M., and Singh,
557 H. B.: Atmospheric budget of acetone, Journal of Geophysical Research-Atmospheres, 107, Artn
558 4100
559 10.1029/2001jd000694, 2002.
560 Jenkin, M. E., Saunders, S. M., and Pilling, M. J.: The tropospheric degradation of volatile
561 organic compounds: A protocol for mechanism development, Atmospheric Environment, 31, 81-
562 104, Doi 10.1016/S1352-2310(96)00105-7, 1997.
563 Jeong, D., Seco, R., Gu, D., Lee, Y. R. O., Nault, B. A., Knote, C. J., Mcgee, T., Sullivan, J. T.,
564 Jimenez, J. L., Campuzano-Jost, P., Blake, D. R., Sanchez, D., Guenther, A. B., Tanner, D.,
565 Huey, L. G., Long, R., Anderson, B. E., Hall, S. R., Ullmann, K., Shin, H. J., Herndon, S. C.,
566 Lee, Y. A. E., Kim, D., Ahn, O. O. Y., and Kim, S.: Integration of airborne and ground
567 observations of nitryl chloride in the Seoul metropolitan area and the implications on regional
568 oxidation capacity during KORUS-AQ 2016, Atmospheric Chemistry and Physics, 19, 12779-
569 12795, 10.5194/acp-19-12779-2019, 2019.
570 Jordan, A., Haidacher, S., Hanel, G., Hartungen, E., Mark, L., Seehauser, H., Schottkowsky, R.,
571 Sulzer, P., and Mark, T. D.: A high resolution and high sensitivity proton-transfer-reaction time-
572 of-flight mass spectrometer (PTR-TOF-MS), International Journal of Mass Spectrometry, 286,
573 122-128, 2009a.
574 Jordan, A., Haidacher, S., Hanel, G., Hartungen, E., Märk, L., Seehauser, H., Schottkowsky, R.,
575 Sulzer, P., and Märk, T. D.: A high resolution and high sensitivity proton-transfer-reaction time-
576 of-flight mass spectrometer (PTR-TOF-MS), Int J Mass Spectrom, 286, 122-128,
577 http://dx.doi.org/10.1016/j.ijms.2009.07.005, 2009b.
578 Kaiser, J., Skog, K. M., Baumann, K., Bertman, S. B., Brown, S. B., Brune, W. H., Crounse, J.
579 D., de Gouw, J. A., Edgerton, E. S., Feiner, P. A., Goldstein, A. H., Koss, A., Misztal, P. K.,
580 Nguyen, T. B., Olson, K. F., St Clair, J. M., Teng, A. P., Toma, S., Wennberg, P. O., Wild, R. J.,
581 Zhang, L., and Keutsch, F. N.: Speciation of OH reactivity above the canopy of an isoprene-

https://doi.org/10.5194/acp-2020-174
Preprint. Discussion started: 24 March 2020

582 dominated forest, Atmospheric Chemistry and Physics, 16, 9349-9359, 10.5194/acp-16-9349-
583 2016, 2016.
584 Kim, S., Karl, T., Guenther, A., Tyndall, G., Orlando, J., Harley, P., Rasmussen, R., and Apel,
585 E.: Emissions and ambient distributions of Biogenic Volatile Organic Compounds (BVOC) in a
586 ponderosa pine ecosystem: interpretation of PTR-MS mass spectra, Atmospheric Chemistry and
587 Physics, 10, 1759-1771, 2010.
588 Kim, S., Guenther, A., Karl, T., and Greenberg, J.: Contributions of primary and secondary
589 biogenic VOC tototal OH reactivity during the CABINEX (Community Atmosphere-Biosphere
590 INteractions Experiments)-09 field campaign, Atmospheric Chemistry and Physics, 11, 8613-
591 8623, 10.5194/acp-11-8613-2011, 2011.
592 Kim, S., Wolfe, G. M., Mauldin, L., Cantrell, C., Guenther, A., Karl, T., Turnipseed, A.,
593 Greenberg, J., Hall, S. R., Ullmann, K., Apel, E., Hornbrook, R., Kajii, Y., Nakashima, Y.,
594 Keutsch, F. N., DiGangi, J. P., Henry, S. B., Kaser, L., Schnitzhofer, R., Graus, M., Hansel, A.,
595 Zheng, W., and Flocke, F. F.: Evaluation of HOx sources and cycling using measurement-
596 constrained model calculations in a 2-methyl-3-butene-2-ol (MBO) and monoterpene (MT)
597 dominated ecosystem, Atmospheric Chemistry and Physics, 13, 2031-2044, Doi 10.5194/Acp-
598 13-2031-2013, 2013a.
599 Kim, S., Kim, S. Y., Lee, M., Shim, H., Wolfe, G. M., Guenther, A. B., He, A., Hong, Y., and
600 Han, J.: Impact of isoprene and HONO chemistry on ozone and OVOC formation in a semirural
601 South Korean forest, Atmospheric Chemistry and Physics, 15, 4357-4371, Doi 10.5194/Acp-15-
602 4357-2015, 2015.
603 Kim, S., Sanchez, D., Wang, M. D., Seco, R., Jeong, D., Hughes, S., Barletta, B., Blake, D. R.,
604 Jung, J., Kim, D., Lee, G., Lee, M., Ahn, J., Lee, S.-D., Cho, G., Sung, M.-Y., Lee, Y.-H., Kim,
605 D. B., Kim, Y., Woo, J. H., Jo, D., Park, R., Park, J. H., Hong, Y.-D., and Hong, J.-H.: OH
606 Reactivity in Urban and Suburban regions in Seoul, South Korea-An East Asia megacity in a
607 rapid transition, Faraday Discussions, DOI:10.1039/C5FD00230C,
608 DOI:10.1039/C1035FD00230C, 2016.
609 Kim, S., Jeong, D., Sanchez, D., Wang, M., Seco, R., Blake, D., Meinardi, S., Barletta, B.,
610 Hughes, S., Jung, J., Kim, D., Lee, G., Lee, M., Ahn, J., Lee, S.-D., Cho, G., Sung, M.-Y., Lee,
611 Y.-H., and Park, R.: The Controlling Factors of Photochemical Ozone Production in Seoul,
612 South Korea, Aerosol Air Qual Res, 18, 2253-2261, 10.4209/aaqr.2017.11.0452, 2018.
613 Kim, S. Y., Jiang, X. Y., Lee, M., Turnipseed, A., Guenther, A., Kim, J. C., Lee, S. J., and Kim,
614 S.: Impact of biogenic volatile organic compounds on ozone production at the Taehwa Research
615 Forest near Seoul, South Korea, Atmospheric Environment, 70, 447-453, Doi
616 10.1016/J.Atmosenv.2012.11.005, 2013b.
617 Koss, A., Yuan, B., Warneke, C., Gilman, J. B., Lerner, B. M., Veres, P. R., Peischl, J.,
618 Eilerman, S., Wild, R., Brown, S. S., Thompson, C. R., Ryerson, T., Hanisco, T., Wolfe, G. M.,
619 Clair, J. M. S., Thayer, M., Keutsch, F. N., Murphy, S., and de Gouw, J.: Observations of VOC
620 emissions and photochemical products over US oil- and gas-producing regions using high-
621 resolution H3O+ CIMS (PTR-ToF-MS), Atmospheric Measurement Techniques, 10, 2941-2968,
622 10.5194/amt-10-2941-2017, 2017.
623 Kovacs, T. A., Brune, W. H., Harder, H., Martinez, M., Simpas, J. B., Frost, G. J., Williams, E.,
624 Jobson, T., Stroud, C., Young, V., Fried, A., and Wert, B.: Direct measurements of urban OH
625 reactivity during Nashville SOS in summer 1999, Journal of Environmental Monitoring, 5, 68-
626 74, 10.1039/b204339d, 2003.

https://doi.org/10.5194/acp-2020-174
Preprint. Discussion started: 24 March 2020

627 Kwok, E. S. C., and Atkinson, R.: Estimation of Hydroxyl Radical Reaction-Rate Constants for
628 Gas-Phase Organic-Compounds Using a Structure-Reactivity Relationship - an Update,
629 Atmospheric Environment, 29, 1685-1695, Doi 10.1016/1352-2310(95)00069-B, 1995.
630 Lee, A., Goldstein, A. H., Kroll, J. H., Ng, N. L., Varutbangkul, V., Flagan, R. C., and Seinfeld,
631 J. H.: Gas-phase products and secondary aerosol yields from the photooxidation of 16 different
632 terpenes, Journal of Geophysical Research-Atmospheres, 111, Artn D17305
633 10.1029/2006jd007050, 2006.
634 Mao, J. Q., Ren, X. R., Chen, S. A., Brune, W. H., Chen, Z., Martinez, M., Harder, H., Lefer, B.,
635 Rappengluck, B., Flynn, J., and Leuchner, M.: Atmospheric oxidation capacity in the summer of
636 Houston 2006: Comparison with summer measurements in other metropolitan studies,
637 Atmospheric Environment, 44, 4107-4115, 10.1016/j.atmosenv.2009.01.013, 2010.
638 Nakashima, Y., Kato, S., Greenberg, J., Harley, P., Karl, T., Turnipseed, A., Apel, E., Guenther,
639 A., Smith, J., and Kajii, Y.: Total OH reactivity measurements in ambient air in a southern
640 Rocky mountain ponderosa pine forest during BEACHON-SRM08 summer campaign,
641 Atmospheric Environment, 85, 1-8, 2014.
642 Nolscher, A. C., Williams, J., Sinha, V., Custer, T., Song, W., Johnson, A. M., Axinte, R.,
643 Bozem, H., Fischer, H., Pouvesle, N., Phillips, G., Crowley, J. N., Rantala, P., Rinne, J.,
644 Kulmala, M., Gonzales, D., Valverde-Canossa, J., Vogel, A., Hoffmann, T., Ouwersloot, H. G.,
645 de Arellano, J. V. G., and Lelieveld, J.: Summertime total OH reactivity measurements from
646 boreal forest during HUMPPA-COPEC 2010, Atmospheric Chemistry and Physics, 12, 8257-
647 8270, Doi 10.5194/Acp-12-8257-2012, 2012.
648 Nolscher, A. C., Yanez-Serrano, A. M., Wolff, S., de Araujo, A. C., Lavric, J. V., Kesselmeier,
649 J., and Williams, J.: Unexpected seasonality in quantity and composition of Amazon rainforest
650 air reactivity, Nature Communications, 7, ARTN 10383
651 10.1038/ncomms10383, 2016.
652 Ortega, J., Turnipseed, A., Guenther, A. B., Karl, T. G., Day, D. A., Gochis, D., Huffman, J. A.,
653 Prenni, A. J., Levin, E. J. T., Kreidenweis, S. M., DeMott, P. J., Tobo, Y., Patton, E. G., Hodzic,
654 A., Cui, Y. Y., Harley, P. C., Hornbrook, R. S., Apel, E. C., Monson, R. K., Eller, A. S. D.,
655 Greenberg, J. P., Barth, M. C., Campuzano-Jost, P., Palm, B. B., Jimenez, J. L., Aiken, A. C.,
656 Dubey, M. K., Geron, C., Offenberg, J., Ryan, M. G., Fornwalt, P. J., Pryor, S. C., Keutsch, F.
657 N., DiGangi, J. P., Chan, A. W. H., Goldstein, A. H., Wolfe, G. M., Kim, S., Kaser, L.,
658 Schnitzhofer, R., Hansel, A., Cantrell, C. A., Mauldin, R. L., and Smith, J. N.: Overview of the
659 Manitou Experimental Forest Observatory: site description and selected science results from
660 2008 to 2013, Atmospheric Chemistry and Physics, 14, 6345-6367, 10.5194/acp-14-6345-2014,
661 2014.
662 Ramasamy, S., Nagai, Y., Takeuchi, N., Yamasaki, S., Shojia, K., Ida, A., Jones, C., Tsurumaru,
663 H., Suzuki, Y., Yoshino, A., Shimada, K., Nakashima, Y., Kato, S., Hatakeyama, S., Matsuda,
664 K., and Kajii, Y.: Comprehensive measurements of atmospheric OH reactivity and trace species
665 within a suburban forest near Tokyo during AQUAS-TAMA campaign, Atmospheric
666 Environment, 184, 166-176, 10.1016/j.atmosenv.2018.04.035, 2018.
667 Ren, X. R., Harder, H., Martinez, M., Lesher, R. L., Oliger, A., Shirley, T., Adams, J., Simpas, J.
668 B., and Brune, W. H.: HOx concentrations and OH reactivity observations in New York City
669 during PMTACS-NY2001, Atmospheric Environment, 37, 3627-3637, 10.1016/S1352-
670 2310(03)00460-6, 2003.
671 Ren, X. R., Brune, W. H., Oliger, A., Metcalf, A. R., Simpas, J. B., Shirley, T., Schwab, J. J.,
672 Bai, C. H., Roychowdhury, U., Li, Y. Q., Cai, C. X., Demerjian, K. L., He, Y., Zhou, X. L., Gao,

https://doi.org/10.5194/acp-2020-174
Preprint. Discussion started: 24 March 2020

Atmospheric Chemistry and Physics Discussions

673 H. L., and Hou, J.: OH, HO2, and OH reactivity during the PMTACS-NY Whiteface Mountain
674 2002 campaign: Observations and model comparison, Journal of Geophysical Research-
675 Atmospheres, 111, Artn D10s03
676 10.1029/2005jd006126, 2006.
677 Rinne, J., Ruuskanen, T. M., Reissell, A., Taipale, R., Hakola, H., and Kulmala, M.: On-line
678 PTR-MS measurements of atmospheric concentrations of volatile organic compounds in a
679 European boreal forest ecosystem, Boreal Environ Res, 10, 425-436, 2005.
680 Sanchez, D., Jeong, D., Seco, R., Wrangham, I., Park, J.-H., Brune, W. H., Koss, A., Gilman, J.,
681 de Gouw, J., Misztal, P., Goldstein, A., Baumann, K., Wennberg, P. O., Keutsch, F. N.,
682 Guenther, A., and Kim, S.: Intercomparison of OH and OH reactivity measurements in a high
683 isoprene and low NO environment during the Southern Oxidant and Aerosol Study (SOAS),
684 Atmospheric Environment, 174, 227-236, 10.1016/j.atmosenv.2017.10.056, 2018.
685 Saunders, S. M., Jenkin, M. E., Derwent, R. G., and Pilling, M. J.: Protocol for the development
686 of the Master Chemical Mechanism, MCM v3 (Part A): tropospheric degradation of non-
687 aromatic volatile organic compounds, Atmospheric Chemistry and Physics, 3, 161-180, 2003.
688 Seco, R., Penuelas, J., and Filella, I.: Short-chain oxygenated VOCs: Emission and uptake by
689 plants and atmospheric sources, sinks, and concentrations, Atmospheric Environment, 41, 2477-
690 2499, 10.1016/j.atmosenv.2006.11.029, 2007.
691 Shirley, T. R., Brune, W. H., Ren, X., Mao, J., Lesher, R., Cardenas, B., Volkamer, R., Molina,
692 L. T., Molina, M. J., Lamb, B., Velasco, E., Jobson, T., and Alexander, M.: Atmospheric
693 oxidation in the Mexico City Metropolitan Area (MCMA) during April 2003, Atmospheric
694 Chemistry and Physics, 6, 2753-2765, DOI 10.5194/acp-6-2753-2006, 2006.
695 Sinha, V., Williams, J., Crowley, J. N., and Lelieveld, J.: The comparative reactivity method - a
696 new tool to measure total OH reactivity in ambient air, Atmospheric Chemistry and Physics, 8,
697 2213-2227, 2008a.
698 Sinha, V., Williams, J., Crowley, J. N., and Lelieveld, J.: The Comparative Reactivity Method
699 – a new tool to measure total OH Reactivity in ambient air, Atmos. Chem. Phys., 8, 2213-
700 2227, 10.5194/acp-8-2213-2008, 2008b.
701 Sinha, V., Williams, J., Lelieveld, J., Ruuskanen, T. M., Kajos, M. K., Patokoski, J., Hellen, H.,
702 Hakola, H., Mogensen, D., Boy, M., Rinne, J., and Kulmala, M.: OH Reactivity Measurements
703 within a Boreal Forest: Evidence for Unknown Reactive Emissions, Environmental Science &
704 Technology, 44, 6614-6620, Doi 10.1021/Es101780b, 2010.
705 Sinha, V., Williams, J., Diesch, J. M., Drewnick, F., Martinez, M., Harder, H., Regelin, E.,
706 Kubistin, D., Bozem, H., Hosaynali-Beygi, Z., Fischer, H., Andres-Hernandez, M. D., Kartal, D.,
707 Adame, J. A., and Lelieveld, J.: Constraints on instantaneous ozone production rates and regimes
708 during DOMINO derived using in-situ OH reactivity measurements, Atmospheric Chemistry and
709 Physics, 12, 7269-7283, Doi 10.5194/Acp-12-7269-2012, 2012.
710 Sullivan, J. T., McGee, T. J., Stauffer, R. M., Thompson, A. M., Weinheimer, A., Knote, C.,
711 Janz, S., Wisthaler, A., Long, R., Szykman, J., Park, J., Lee, Y., Kim, S., Jeong, D., Sanchez, D.,
712 Twigg, L., Sumnicht, G., Knepp, T., and Schroeder, J. R.: Taehwa Research Forest: a receptor
713 site for severe domestic pollution events in Korea during 2016, Atmospheric Chemistry and
714 Physics, 19, 5051-5067, 10.5194/acp-19-5051-2019, 2019.
715 Whalley, L. K., Stone, D., Bandy, B., Dunmore, R., Hamilton, J. F., Hopkins, J., Lee, J. D.,
716 Lewis, A. C., and Heard, D. E.: Atmospheric OH reactivity in central London: observations,
717 model predictions and estimates of in situ ozone production, Atmospheric Chemistry and
718 Physics, 16, 2109-2122, 10.5194/acp-16-2109-2016, 2016.

https://doi.org/10.5194/acp-2020-174
Preprint. Discussion started: 24 March 2020

Atmospheric Chemistry and Physics Discussions

719 Williams, J., Poschl, U., Crutzen, P. J., Hansel, A., Holzinger, R., Warneke, C., Lindinger, W.,
720 and Lelieveld, J.: An atmospheric chemistry interpretation of mass scans obtained from a proton
721 transfer mass spectrometer flown over the tropical rainforest of Surinam, Journal of Atmospheric
722 Chemistry, 38, 133-166, Doi 10.1023/A:1006322701523, 2001.
723 Yang, Y. D., Shao, M., Wang, X. M., Nolscher, A. C., Kessel, S., Guenther, A., and Williams, J.:
724 Towards a quantitative understanding of total OH reactivity: A review, Atmospheric
725 Environment, 134, 147-161, 10.1016/j.atmosenv.2016.03.010, 2016.
726 Yang, Y. D., Shao, M., Kessel, S., Li, Y., Lu, K. D., Lu, S. H., Williams, J., Zhang, Y. H., Zeng,
727 L. M., Noelscher, A. C., Wu, Y. S., Wang, X. M., and Zheng, J. Y.: How the OH reactivity
728 affects the ozone production efficiency: case studies in Beijing and Heshan, China, Atmospheric
729 Chemistry and Physics, 17, 7127-7142, 10.5194/acp-17-7127-2017, 2017.
730 Yuan, B., Warneke, C., Shao, M., and de Gouw, J. A.: Interpretation of volatile organic
731 compound measurements by proton-transfer-reaction mass spectrometry over the deepwater
732 horizon oil spill, International Journal of Mass Spectrometry, 358, 43-48,
733 10.1016/j.ijms.2013.11.006, 2014.
734 Zannoni, N., Gros, V., Esteve, R. S., Kalogridis, C., Michoud, V., Dusanter, S., Sauvage, S.,
735 Locoge, N., Colomb, A., and Bonsang, B.: Summertime OH reactivity from a receptor coastal
736 site in the Mediterranean Basin, Atmospheric Chemistry and Physics, 17, 12645-12658, 2017.
737 Zhao, J., Zhang, R. Y., Fortner, E. C., and North, S. W.: Quantification of hydroxycarbonyls
738 from OH-isoprene reactions, J Am Chem Soc, 126, 2686-2687, 10.1021/ja0386391, 2004.
739

740

741

742

743 **Tables and Figures**

744

745 Table 1. Description of instrument and measured parameters.

Instrument	**Parameters**	**Measurement Uncertainty (1σ)**
Chemical Ionization Spectroscopy - Comparative Reactivity Method - (CIMS-CRM)	OH reactivity	16.7%
Thermo Scien8fic 42i	NO	20%
Cavity Ring Down Spectroscopy	NO_2	20%
Thermo Scientific 49i	O_3	4%
Lufft 501 C	Temperature	±0.3 °C
Thermo Scientific 48i TLE	CO	10%
Thermo Scientific 43i TLE	SO_2	10%

https://doi.org/10.5194/acp-2020-174
Preprint. Discussion started: 24 March 2020

Atmospheric Chemistry and Physics Discussions

Mini Tunable Infrared Laser Direct Absorption Spectroscopy (mini-TILDAS) Formaldehyde Monitor	HCHO, CH_4, CH_3OH	5%
Proton Transfer Reaction Time of Flight Mass Spectrometer (PTR-TOF-MS)	Acetaldehyde, Ethanol, Acetone, Isoprene, MVK + MACR, Methyl ethyl ketone, Benzene, Monoterpenes, Toluene, Furfural, Benzaldehyde, Xylenes, Trimethylbenzenes, Sesquiterpenes	Isoprene 9.8% Benzene 6.9% Toluene 6.5% Monoterpenes 9.2% Xylenes 4.0% Other 16.5%

746

747

748

749

750

751

https://doi.org/10.5194/acp-2020-174
Preprint. Discussion started: 24 March 2020

Atmospheric Chemistry and Physics Discussions

752

753

754 Figure 1. Observed and calculated OH reactivity during KORUS-AQ 2016. The measured and

755 calculated OH reactivity are on the left axis while the missing OH reactivity is on the right axis.

756 The yellow box represents the stagnation period and the blue box represents the transport period.

757

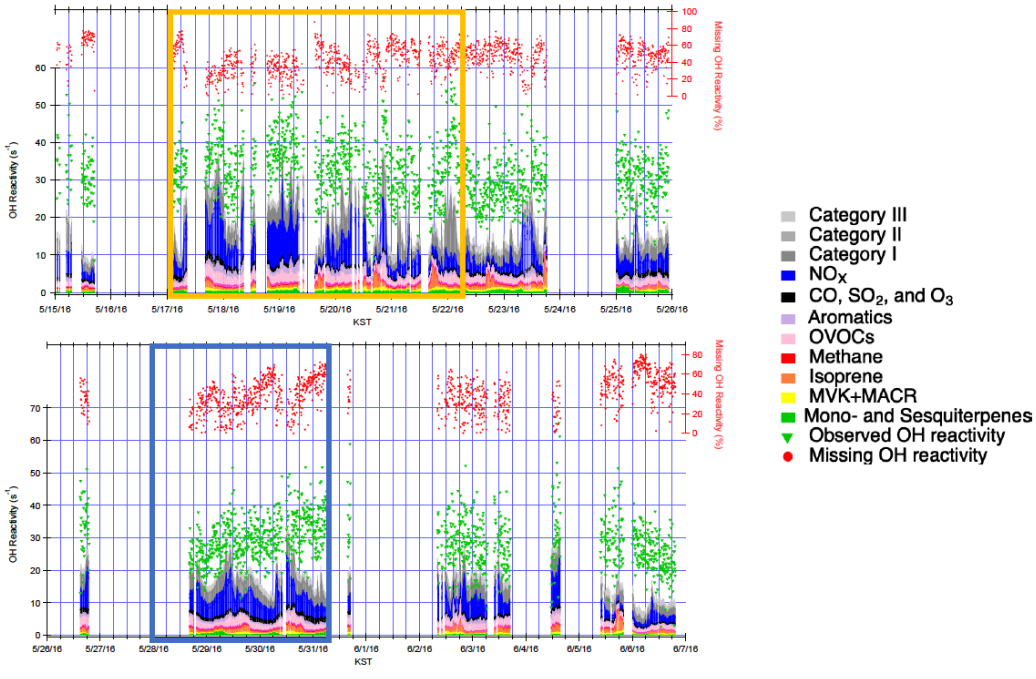

758

https://doi.org/10.5194/acp-2020-174
Preprint. Discussion started: 24 March 2020

Atmospheric Chemistry and Physics Discussions

759

760 Figure 2. The diurnal average of OH reactivity from 15 May 2016 – 7 June 2016. The measured
761 and calculated OH reactivity are on the left axis. The blue shading represents uncertainty in the
762 measured OH reactivity. The black bars represent the propagated uncertainty of calculated OH
763 reactivity. The missing OH Reactivity in the percentage scale can be read using the right axis.

764

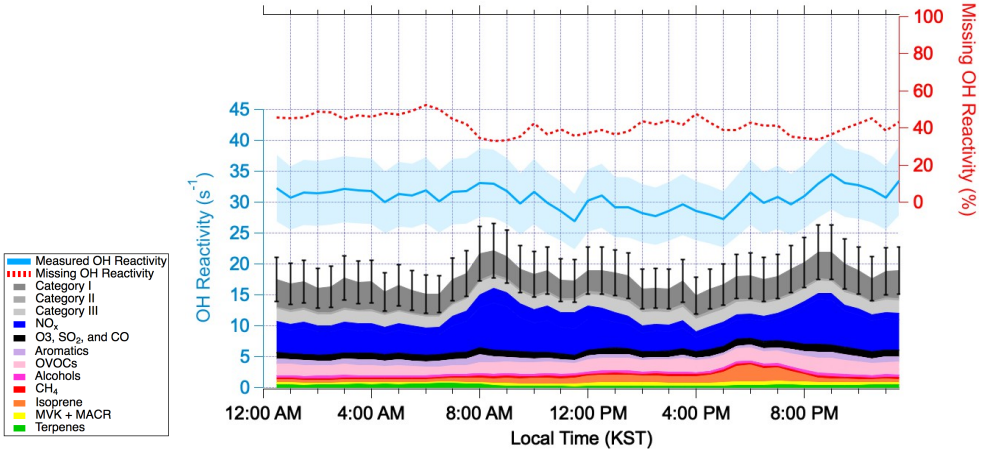

765

766

767

768

769

770

771

772

773

774

775

https://doi.org/10.5194/acp-2020-174
Preprint. Discussion started: 24 March 2020

Atmospheric Chemistry and Physics Discussions

776

777 Figure 3. Diurnal averages of OH reactivity during the stagnation period (A) from May 17th –
778 May 22nd in 2016 and the transport period (B) from 28 May – 1 June 2016. The measured and
779 calculated OH reactivity are on the left. The blue shading represents an uncertainty of 16.7% at
780 1σ. The black bars represent the propagated uncertainty of 20.1% at 1σ from calculated missing
781 OH reactivity. The percent missing OH reactivity is on the right axis.

782

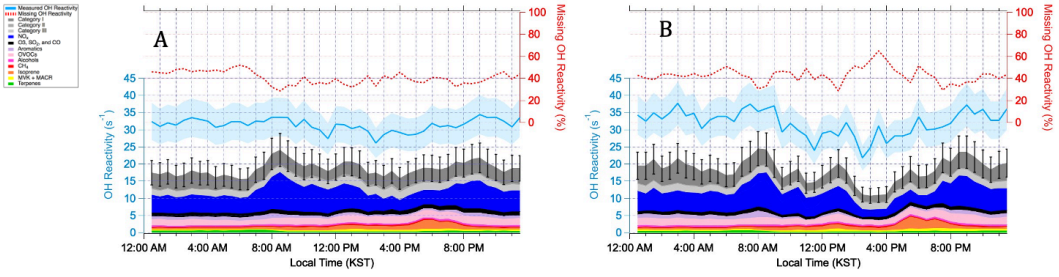

783

784

785

786

787

788

789

790

791

792

793

https://doi.org/10.5194/acp-2020-174
Preprint. Discussion started: 24 March 2020

Atmospheric Chemistry and Physics Discussions

794

795

796 Figure 4. The observed OH reactivity during the overall campaign, stagnation period, and

797 transport period.

798

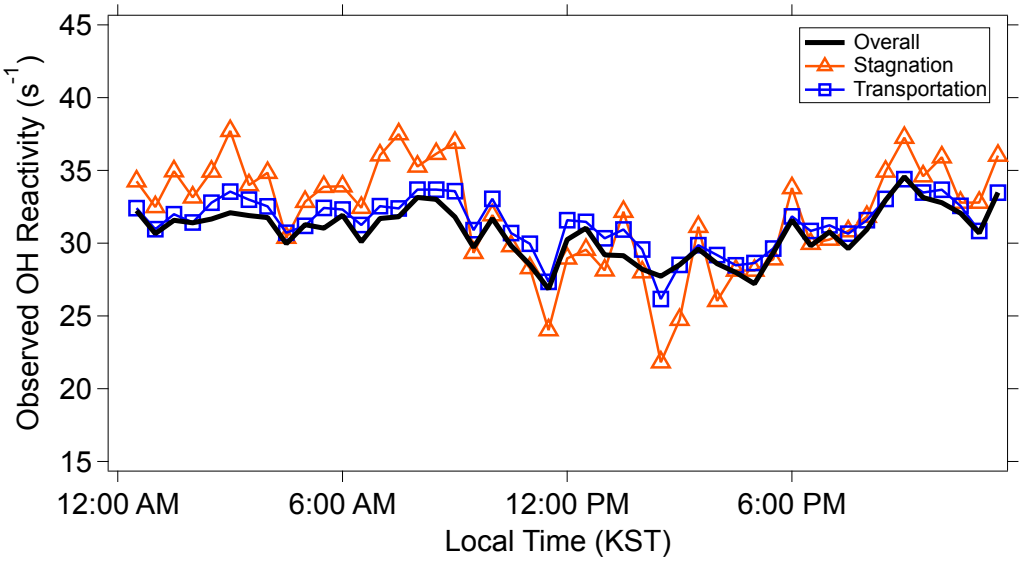

799

800

801

802

803

804

805

806

807

808

https://doi.org/10.5194/acp-2020-174
Preprint. Discussion started: 24 March 2020

Atmospheric Chemistry and Physics Discussions

809

810 Figure 5. Diurnal profiles for different classes of trace gases during the different periods. A)

811 criteria pollutants NO_x, O_3, SO_2, and CO B) Aromatics, C) BVOCs, and D) OVOCs

812

813

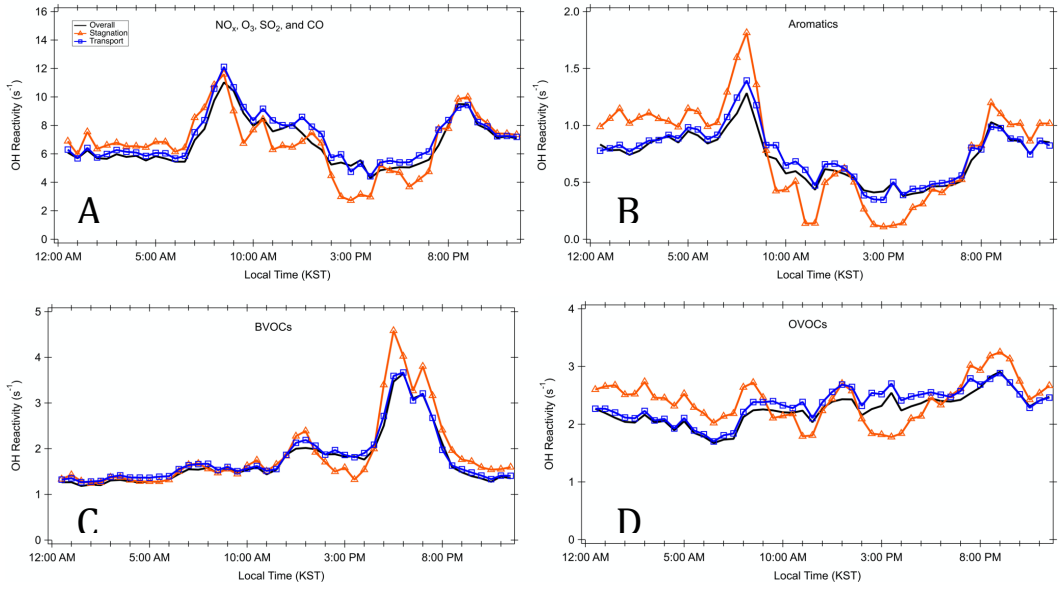

814

815

816

817

818

819

820

821

822

823

https://doi.org/10.5194/acp-2020-174
Preprint. Discussion started: 24 March 2020

Atmospheric Chemistry and Physics Discussions

824

825 Figure 6. Diurnal averages of the OH reactivity from the compounds in A) Category I, B)

826 Category II and C) Category III

827

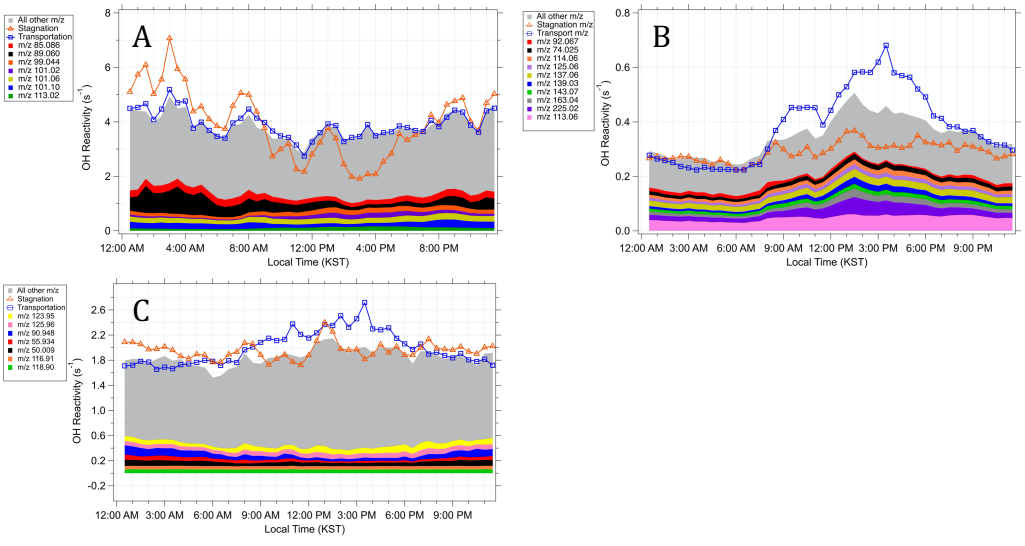

828

829

830

831

832

833

834

835

836

837

838

839

https://doi.org/10.5194/acp-2020-174
Preprint. Discussion started: 24 March 2020

Atmospheric Chemistry and Physics Discussions

840

841 Figure 7. The correlation between A) NOx OH reactivity and absolute missing OH reactivity and

842 B) percent missing OH reactivity

843

844

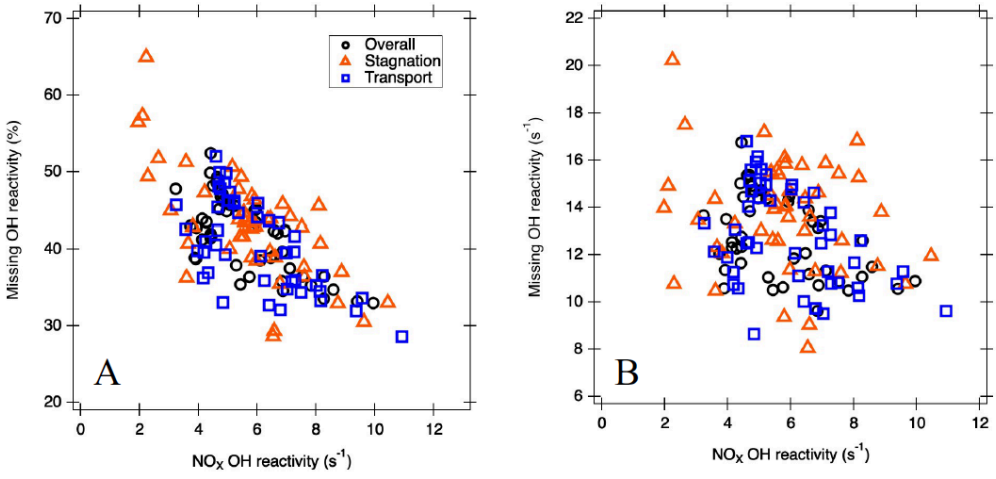

845